Hindawi
Advances in Civil Engineering
Volume 2023, Article ID 5515450, 16 pages
https://doi.org/10.1155/2023/5515450

Research Article

Vibration Analysis of Low Height-to-Span Ratio Pedestrian Bridge under Human-Induced Excitation

Wei Wang,[1] Rui An,[2] Huihui Huang ,[3] Jie Li ,[1] Jinghang Niu ,[1] Huan Liao ,[1] Jian Jiao,[1] Zhiqiang Li ,[1] and Yuekai Tao[1]

[1]*College of Water Conservancy & Architectural Engineering, Shihezi University, Shihezi 832003, China*
[2]*Shanghai Municipal Engineering Design and Research Institute Group Xinjiang Co., Ltd., Urmuqi 830000, China*
[3]*Guangdong Architectural Design & Research Institute Co., Ltd., Guangzhou 510010, China*

Correspondence should be addressed to Huihui Huang; 475910361@qq.com, Jie Li; 18245526@qq.com, Jinghang Niu; niujinghang@126.com, Huan Liao; shzu_sj_lh@163.com, and Zhiqiang Li; zhiqiangli2023@163.com

Received 19 April 2023; Revised 11 May 2023; Accepted 12 May 2023; Published 13 June 2023

Academic Editor: Carlo Rainieri

Driven by the aesthetic pursuit of the urban landscape, pedestrian bridges become longer, lighter, and slender, which may be susceptible to unacceptable vibrations induced by human activities. This paper presented on-site vibration tests of a pedestrian bridge with a very low height-to-span ratio (1/60). The vibration characteristics and dynamic responses were analyzed using environmental, heel-drop, and walking tests. Then, a verified finite model was established to investigate the effect of the height-to-span ratio and the concrete filling ranges of tree-like steel piers on the vibration characteristics and acceleration responses of this kind of pedestrian bridges. Moreover, the relationship between different peak accelerations under heel-drop and walking at various frequencies by the same person was detailed and studied experimentally and by computer simulation, after which the ratios of the peak acceleration during walking and the one under heel-drop were recommended. Finally, a method that demonstrates the feasibility of predicting the peak acceleration of pedestrian bridges of a small height-to-span ratio across a range of walking frequencies was proposed based on a simplified heel-drop load model developed according to 60 time-history records.

1. Introduction

Pedestrian bridges serve as vital elements of urban transportation infrastructure, enabling the safe and efficient movement of individuals across various urban landscapes [1]. In recent years, incidents of human-induced vibrations on pedestrian bridges have been reported globally [2, 3]. For instance, the Millennium Bridge in London [4], the Kurilpa Bridge in Brisbane [5], and the Bob Kerrey Pedestrian Bridge in Omaha [3] have all experienced significant vibrations due to their small height-to-span ratios and exposure to human-induced loads [6, 7]. As the design methods of pedestrian bridges continue to evolve, with increasing emphasis on lightweight and large-span structures, understanding the influence of human-induced loads is of paramount importance for ensuring the safety and comfort of pedestrians [8].

Various excitation techniques exist for evaluating the dynamic properties of pedestrian bridges, with heel-drop tests being a widely used method over the years [9]. Heel-drop loads are impact loads generated when a pedestrian's feet strike the ground [10]. The AISC Design Guide 11 [11] outlined a typical heel-drop test, which involved an individual lifting their heels approximately 80 mm from the ground and striking the ground with both heels while avoiding multiple impacts and preventing forward rocking or bouncing on the balls of their feet. Ohmart [12] documented heel-drop impact loading from individuals with an average weight of 85 kg, with a loading duration of 0.05 s. To simplify the load from a heel-drop impact test, Murray [13] proposed a triangular load function. The ratio of peak load F_{peak} to static load Gave is approximately 3.14, with F_{peak} equal to 2670 N and Gave equal to 850 N. These loads could generate substantially greater force peaks and accelerations, potentially causing excessive vibrations and structural safety concerns [14]. However, since Murray's triangular load function was primarily derived from a specific set of test data, this model tends to overestimate the peak acceleration response of pedestrian bridges. Therefore, it is essential to accurately study the effect of heel-drop loads on the vibration acceleration response of pedestrian bridges.

Structural engineers and biomechanics use direct or indirect measurement data to develop accurate force models to evaluate the vibration serviceability of structures such as footbridges and long-span floors. Bedon [15] conducted on-site vibration experiments and a finite element (FE) numerical study to investigate the footbridge sensitivity. Venuti et al. [16] proposed a vertically oriented modeling framework to simulate the time-varying position and velocity of each pedestrian on a footbridge by measuring the footfall forces. Muhammad and Reynolds [17] presented a probabilistic walking load model that generates synthetic vertical load waveforms induced by pedestrians. Mohammed et al. [18] used a comprehensive database of walking force-time histories to develop an improved version of this force model. Van Nimmen et al. [19] and Caprani et al. [20] applied a detailed model to investigate the dynamic response of footbridges to pedestrian excitation. Shahabpoor et al. [21] proposed a new method based on the actual level of vibration experienced by each pedestrian for serviceability assessment of the vertical vibrations induced by pedestrian walking traffic. Middleton et al. [22] reviewed the process of estimating the response to footfalls and proposed simplifying a footfall force-time history for use in design, which has been the subject of research for many years. Santos et al. [23] presented a simplified expression based on the results of an experimental campaign, several numerical analyses, and a theoretical analysis to guarantee that excessive vibrations will not occur, without the need to perform a dynamic analysis.

The pedestrian bridge, with a small height-to-span ratio (1/60) and tree-like steel tube concrete columns, was selected for the investigation. In this study, the experimental and numerical work includes the following:

(1) The acceleration time-history responses and vibration characteristics of a pedestrian bridge under environment, heel-drop, and walking excitations were obtained.

(2) A refined finite element model was established and validated compared to the measured data. Based on the model, parametric analysis was conducted with different height-to-span ratios (1/20–1/80) and concrete filling ranges of tree-like columns (5 filling ranges), investigating the vibration characteristics and peak accelerations under heel-drop excitations.

(3) A simplified heel-drop load model was proposed based on the relationship between a human-body weight and the load peak.

(4) Coefficients, correlating the peak acceleration under the heel-drop excitations with that under the walking excitations of different frequencies (1.7 Hz, 2.0 Hz, 2.3 Hz), were proposed to predict peak structural responses at different walking frequencies.

2. Vibration Experiments

2.1. Project Overview. The pedestrian bridge of this study has a unique design that consisted of tree-like steel tube concrete columns and steel box beam with a span of 30 m. The steel bridge of the bridge span was meticulously crafted a single-box beam with multichamber section boxes made of Q345E steel, which measured $3850\,\text{mm} \times 500\,\text{mm} \times 20\,\text{mm} \times 30\,\text{mm}$ in terms of depth, width, web thickness, and flange thickness, respectively. The bridge was equipped with three internal longitudinal stiffeners and internal transverse stiffeners that were spaced at 4-meter intervals, as depicted in Figure 1(a).

The deck of the bridge was constructed using 80 mm-thick concrete with a strength grade of C20, which was reinforced by a wire mesh comprised of 4 reinforcing bars that were bi-directionally spaced at 150 mm intervals. The main transverse keel was created using an H-section measuring $150\,\text{mm} \times 100\,\text{mm} \times 6\,\text{mm} \times 9\,\text{mm}$ in terms of depth, flange width, web thickness, and flange thickness, respectively. This section was welded to the main steel box beam. Its lower part was embedded in concrete while the upper part was exposed with an interval of 80 mm (Figures 1(a) and 1(b)). The bridge deck was paved with 140 mm wide and 40 mm thick carbonized anticorrosion wood panels, which were fixed using countersunk head screws. The bridge was supported by tree-like concrete-filled steel tubular columns (Figure 1(c)) on both sides. Figure 1(d) shows the depiction of the test pedestrian bridge and its related bridge elements.

2.2. Measurement and Excitations. The placement of vertical accelerometers and the walking path during testing were described in Figure 2(a). The test apparatus consisted of two integral components: the measurement system and the data acquisition system. The measurement system consisted of 14 vertical accelerometers (DH610V) and a force plate. These accelerometers had a measurement range of ± 5 g and minimum sensitivity of 0.01 V/g, where "g" represents the acceleration due to gravity. The sensor was placed on the test rig to collect only vertical acceleration, and the accelerometer was chosen based on the most convenient trade-off between price and self-noise level [24, 25]. The force plate was made up of a high-precision load sensor (type ME-K3D160 with dimensions of $160\,\text{mm} \times 160\,\text{mm} \times 66\,\text{mm}$) and two Q345 steel plates ($500\,\text{mm} \times 400\,\text{mm} \times 25\,\text{mm}$). The load sensor, which had a measuring range of ± 5 kN in the vertical direction, was installed between the two steel plates using 8 bolts.

A data acquisition system, DH5922N, was used to gather all data from the accelerometers and the force plate. This system was capable of acquiring data at a frequency of 1000 Hz, and the systematic resolution of vibration acceleration is $1 \times 10^{-6}\,\text{m/s}^2$. Five participants, including four males and one female, took part in the test. The weight and

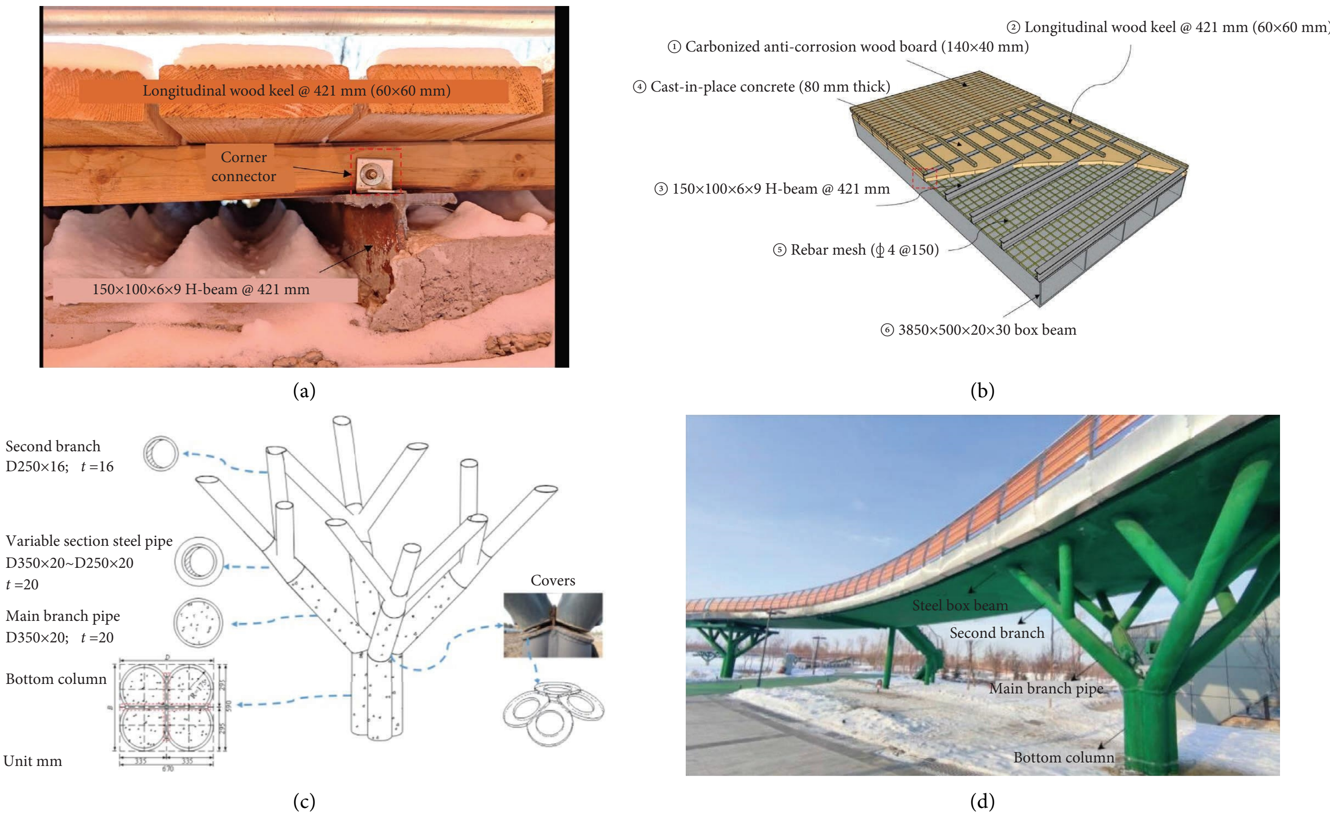

Figure 1: (a) Bridge superstructure details, (b) bridge span structure, (c) tree pier and column structure, and (d) test pedestrian bridge.

height of each tester were presented in Table 1. The average weight recorded was 70.2 kg and the average height was 169 cm. The age of the volunteers participating in this test ranged from 38 to 45 years. These values are significantly lower than the average weight and height of American individuals, making it a noteworthy study to investigate the accelerated response that is induced by human loading at these lighter weights.

The testers underwent a series of heel-drop exercises to ensure uniformity in their heel-drop loads and enhance the accuracy of the test results (Figure 2(b)). They stood on the force plate and performed three consecutive heel-drop at the mid-span (near A_8) and 1/4-span (near A_7) positions with a 15-second interval between each excitation. As a result, thirty sets of heel-drop data were collected to establish the relationship between the peak acceleration response of the bridge under heel-drop excitations and walking excitations. Additionally, sixty sets of heel-drop load data were collected on a rigid ground to provide typical force-time responses for a simplified heel-drop load model, as shown in Figures 3(a) and 3(b).

Walking excitations, the most prevalent load on pedestrian bridges [26], were recorded through tests involving 5 testers who walked for 5 minutes each at common frequencies at frequency of 1.7 Hz, 2.0 Hz, 2.3 Hz, or random step frequency (Figure 2(c)). This resulted in 20 sets of walking excitations tests (4 tests with different step frequencies/person × 5 persons). Figure 3(c) displays the standard acceleration time history responses during a walking excitation. To further understand the impact of walking on pedestrian bridges, an accelerometer was used to collect a total of 350 minutes of acceleration data during a tester walk, as shown in Figure 3(c).

Environmental excitations affecting the pedestrian bridge were primarily caused by airflow (such as wind) and external vibrations (such as the rumbling of vehicles traveling beneath the bridge or ongoing construction work) [27]. No deliberate excitations were necessary to produce these effects. During the 50-minute experiment, the bridge's acceleration responses at different locations were recorded. The typical acceleration time history responses of the collected data are shown in Figures 3(a) to 3(d).

3. Experimental Results

3.1. Frequency. The fast Fourier transform (FFT) technique [28] was used to convert the acceleration response signal of the pedestrian bridge under the heel-drop and walking loads to the frequency domain signal. The fundamental frequency of the pedestrian bridge was identified as 3.35 Hz from the typical spectrum, as shown in Figure 4(a). The results of the tests indicated that the fundamental frequency of the pedestrian bridge could be accurately reflected by both the heel-drop and walking loads. However, the long duration and narrow bandwidth of the walking load generated multiple-order harmonics and high-frequency components in the frequency domain, making it challenging to

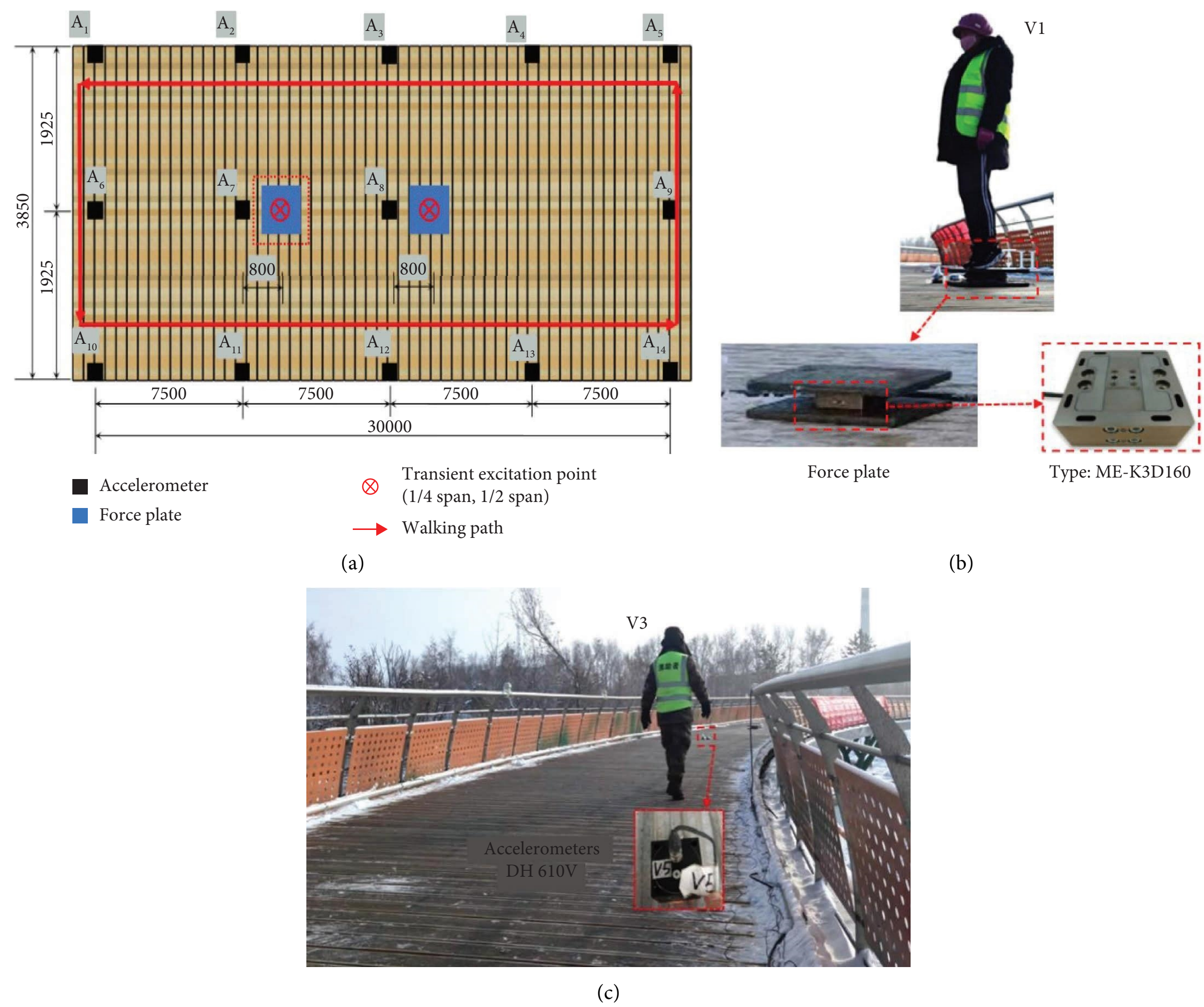

Figure 2: (a) Accelerometer arrangement and walking path, (b) heel-drop, and (c) walking.

Table 1: Tester information.

Tester number	V1	V2	V3	V4	V5
Gender	Female	Male	Male	Male	Male
Weight (kg)	59	65	82	85	60
Height (cm)	158	170	171	176	169

distinguish the fundamental frequency of the bridge [29]. On the other hand, the heel-drop load, which is equivalent to an impact force with a shorter duration and wider bandwidth in the time domain, clearly revealed the bridge's fundamental frequency in the frequency domain.

To further validate the accuracy of the fundamental frequency obtained from heel-drop and walking tests, the environmental excitations of the pedestrian bridge were meticulously analyzed for a continuous 30-minute span using the random subspace identification method [30]. Preset tolerance: characteristic frequency less than 1%, damping ratio less than 5%, and vibration type MAC more than 95%. The results revealed that the fundamental frequency of the pedestrian bridge was 3.35 Hz, and the damping ratio was 0.018, as shown in Figure 4(b). Considering that the vertical fundamental frequencies of large-span pedestrian bridges typically fall within the range of 2–8 Hz [31], it was determined that the heel-drop load was a more suitable method for identifying the vertical fundamental frequency.

3.2. Damping Ratio. Damping is another important parameter in evaluating vibrations, which is related to the energy dissipation of a bridge [32]. The half-power bandwidth method [33] was used to estimate the damping ratio by finding the bandwidth for each mode. This methodology was based on normalizing $\Delta\omega$ the bandwidth across the resonant response, where the amplitude was $0.707R_{\max}$ (Figure 5(a)). The damping ratio could be obtained by the following equation:

$$\xi = \frac{f_2 - f_1}{2f_0}. \tag{1}$$

In Figures 5(b) and 5(c), the mean value, the standard deviation, and the coefficient of variation are abbreviated as MEAN, STD, and CV. The average damping ratio under the walking load was 0.022, with a standard deviation of 0.0077,

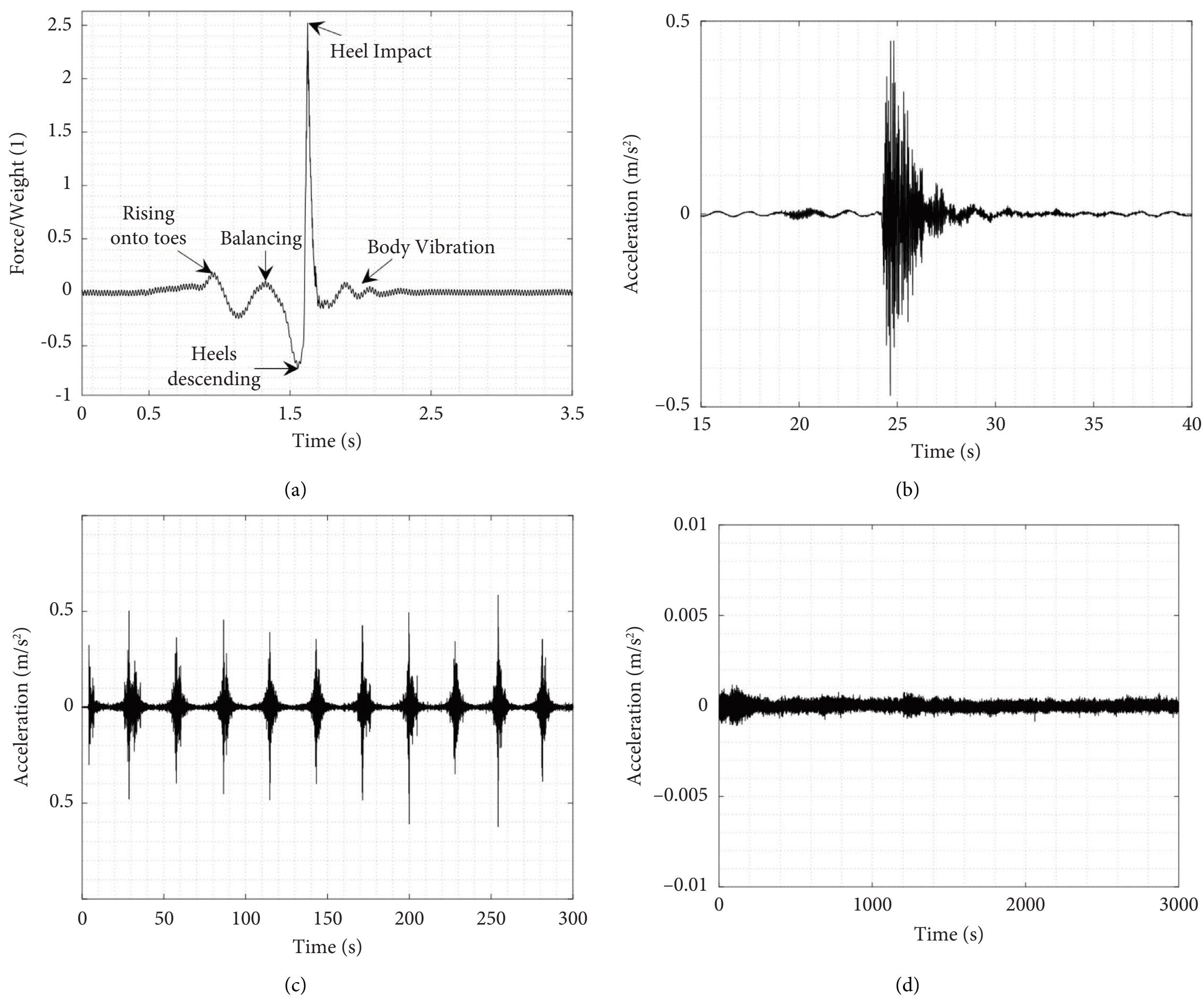

Figure 3: (a) Heel-drop load time history, (b) acceleration time history under heel-drop, (c) acceleration time history under walking, and (d) acceleration time history under environmental excitations.

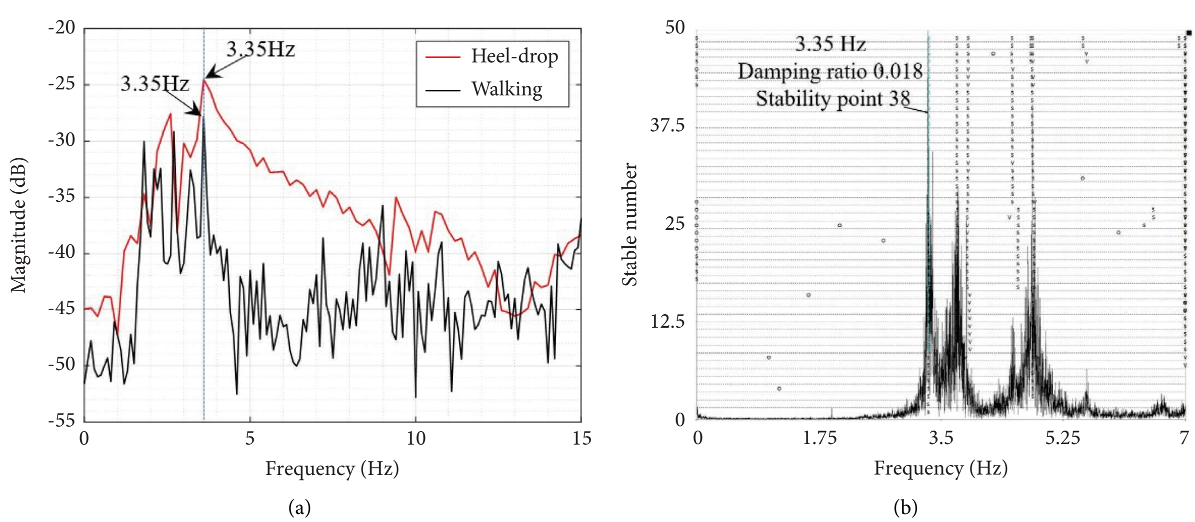

Figure 4: (a) Heel-drop and walking spectrogram and (b) random subspace identification under environmental excitations.

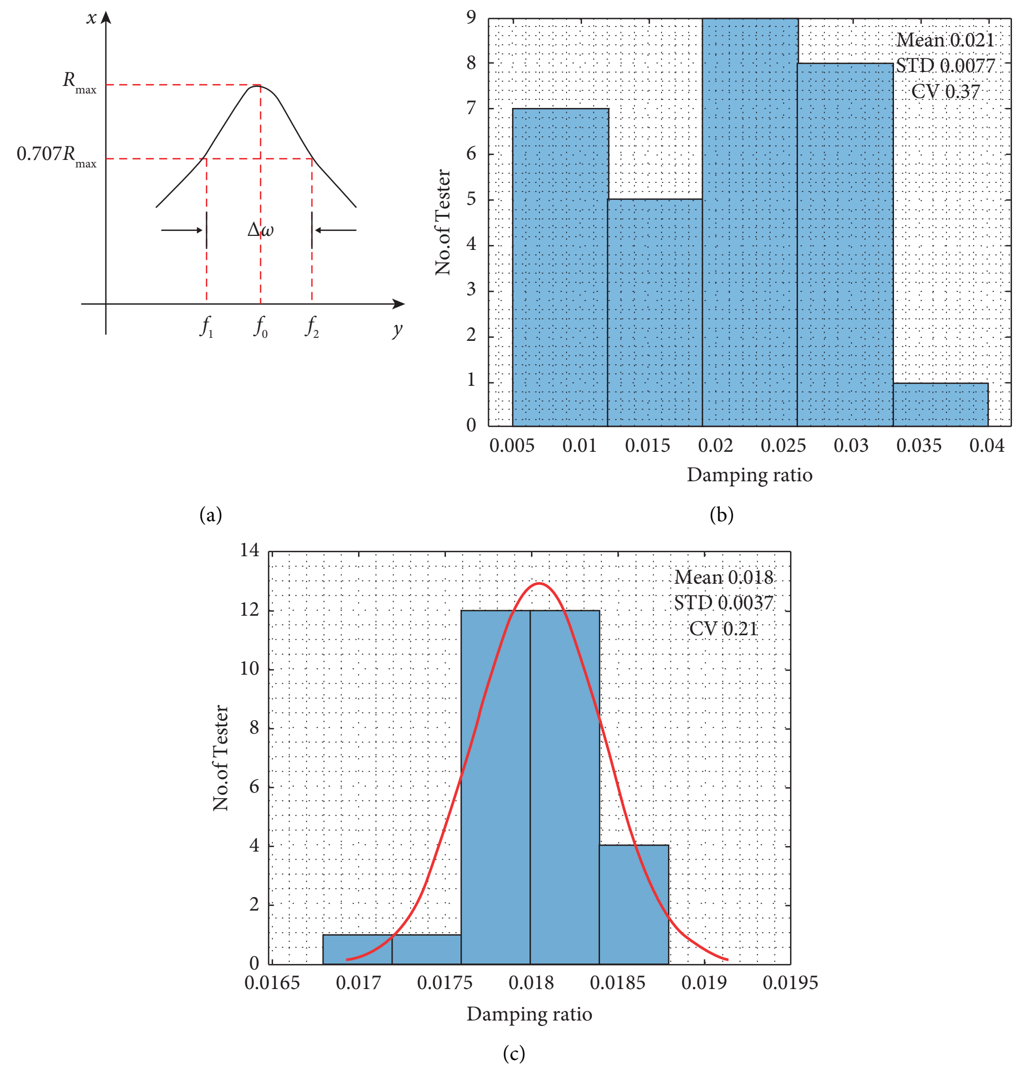

Figure 5: (a) Amplitude-frequency characteristic curve, (b) histogram of damping ratio distribution under walking, and (c) histogram of damping ratio distribution under heel-drop.

as shown in Figure 5(a). Meanwhile, the average damping ratio measured under the heel-drop load was 0.018 with a standard deviation of 0.0037, as shown in Figure 5(b). It was observed that the average damping of the heel-drop test was 18% lower than that of the walking test. This is because the temporal dynamics of the walking load affected the damping of the pedestrian bridge. The coupling effects of stride and gait among different pedestrians, as well as between the pedestrians and the bridge, result in fluctuations and variations in the damping ratios that are measured under walking loads. In comparison to the walking excitations, the damping obtained from the heel-drop excitations was more stable. The use of heel-drop loads in the tests was found to be a more accurate reflection of the bridge's damping characteristics than the use of walking loads. This was primarily due to the fact that heel-drop loads induced a greater impact, providing a more comprehensive assessment of the bridge's ability to absorb and dissipate energy [34].

3.3. Vibration Response. The pedestrian bridge has a range of fundamental frequencies that are generally required to be greater than 5 Hz or to avoid sensitive frequency intervals such as 1.6 to 2.4 Hz and 3.5 to 4.5 Hz [35]. The vertical fundamental frequency of this footbridge is close to the 3 Hz frequency limit specified in the CJJ-69 code [36], and it is necessary to consider its dynamic response under human-induced load excitations. The result of cloud plotting the peak accelerations recorded by the full-span accelerometer showed that the values of adjacent measurement points in the span direction of the pedestrian bridge decreased by 94.58% and 94.16%, respectively, compared to the mid-span point. Similarly, the values of adjacent measurement points in the width direction of the pedestrian bridge decreased by 89.91% and 87.32%, respectively, compared to the mid-span point, as shown in Figure 6(a).

When the heel-drop load was applied at the 1/4-span position, a similar attenuation trend was observed. The values of the adjacent measurement points in the span

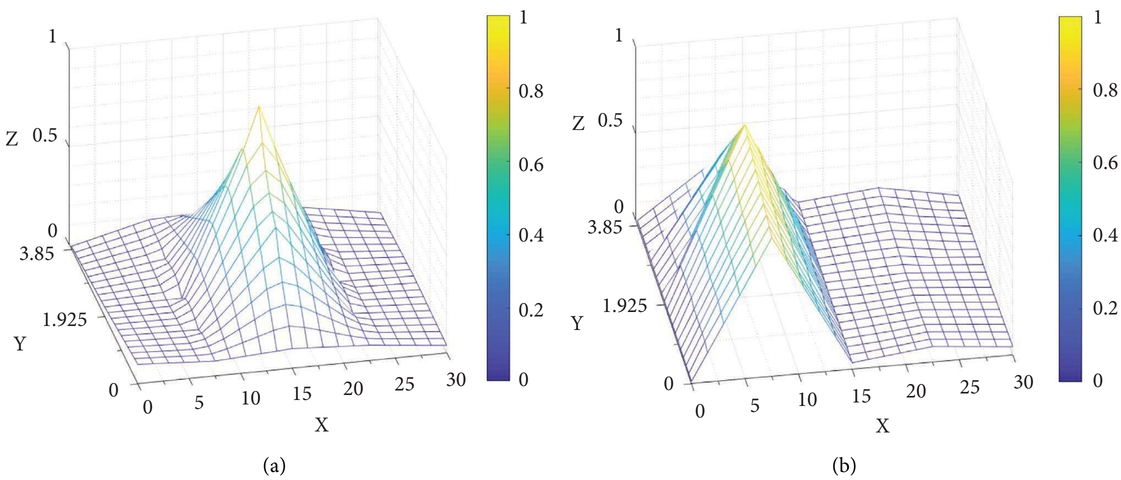

Figure 6: (a) Cloud of peak response distribution of heel-drop excitations of the pedestrian bridge at mid-span position (unit in m) and (b) cloud of peak response distribution of heel-drop excitations of the pedestrian bridge at 1/4 span position (unit in m).

direction of the pedestrian bridge were reduced by 95.47% and 97.86%, respectively, compared to the 1/4-span point, and by 19.74% and 65.11%, respectively, in the width direction, as shown in Figure 6(b).

The results indicated that when the pedestrian bridge is subjected to human-induced loads at different locations, the acceleration attenuate rate at the mid-point of the pedestrian bridge span is slower than that at the 1/4 span, and the acceleration attenuate rate in the pedestrian bridge width direction is also slower.

3.4. Comparison of the Results with the Vibration Acceptability Criteria. Different countries have their own standards for vibration serviceability of footbridges. According to ISO 10137, the vertical vibration (Z-axis) of a footbridge should not exceed a reference curve multiplied by a factor of 60 for the design working life under pedestrian traffic conditions. The Swedish standard BRO20042 specifies that the vertical fundamental frequency of a pedestrian bridge should be greater than 3.5 Hz to ensure vibration comfort for normal use; otherwise, the bridge span should be checked to verify that the vertical root mean square velocity caused by the pedestrian load is less than 0.5 m/s^2.

The average MTVV (mean time-varying velocity) of the bridge structure under heel-drop excitation was 0.082 m/s^2. Figure 7 compares the average MTVV of the heel-drop test with the ISO and BRO limits. The black curve in the figure is the ISO limit range, and the red dashed line is the Bro limit. The peak MTVV of the structure is 0.122 m/s^2, which is much lower than the standard limit.

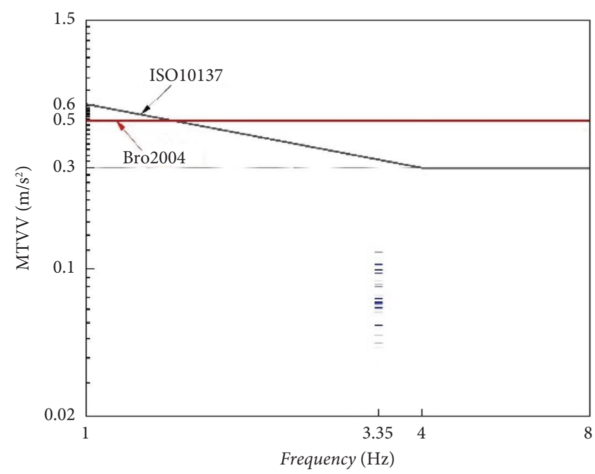

Figure 7: Evaluation of pedestrian-induced dynamic responses.

4. Finite Element Analysis

4.1. Model Establishing. The pedestrian bridge with tree-like columns was modeled using the ABAQUS finite element software. Steel box beams and tree-like columns were modeled with shell element S4R and concrete with solid element C3D8R. The interaction between the steel tube and concrete was simulated through face-to-face contact. Normal and tangential directions were simulated using hard contact and penalty function, respectively, and the friction coefficient between steel and concrete was set as 0.6 [37]. The grid size of the steel box beam was 1/18 of the side length of the section width, while the grid size for the concrete inside the tube was approximately 1/12 of the trunk width of the tree-like columns [38], as depicted in Figure 8(a). The bottom end of the tree-like column was fixed, with U1 = U2 = U3 = UR1 = UR2 = UR3 = 0 [39]. The material properties of the pedestrian bridge, such as density, modulus of elasticity, and Poisson's ratio, are listed in Table 2.

4.2. Model Validation. The initial analysis step is used to define the boundary conditions, and the default parameters are used. The "linear regression-frequency" analysis step is used to calculate the self-oscillation frequency and the corresponding vibration pattern of the model. Note that the Lanczos algorithm is used in the eigenvalue solver to calculate the frequencies, and the state of geometric nonlinearity is set to "off". The "dynamic, implicit" analysis step

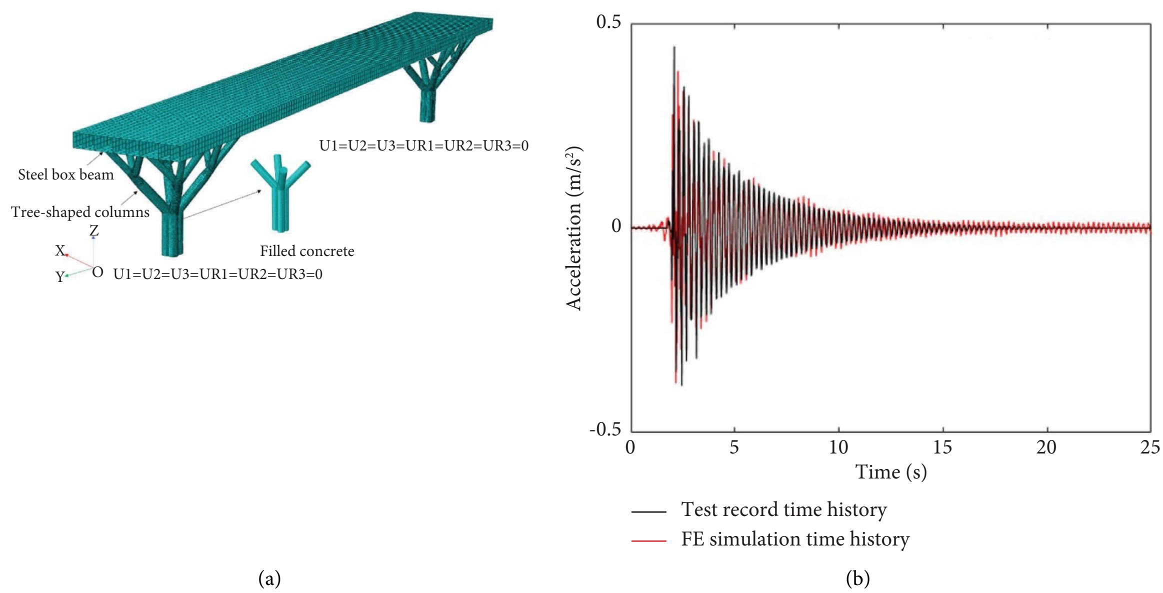

Figure 8: (a) Finite element model and (b) comparison of acceleration time history under heel-drop excitations.

Table 2: Material properties of pedestrian bridges.

Element	ρ (kg/m^3)	E (GPa)	v
Concrete	2450	30.5	0.2
Reinforcement	7850	200	0.3

is used to define the load. For the so-described FE components, a key role was assigned to boundaries, constraints, and material mechanical properties, so as to reproduce the real structural system [40]. Through actual measurement results, it was found that the fundamental frequency of the pedestrian bridge obtained from the finite element model had an error of less than 3% when compared with the test result, as shown in Table 3. Figure 8(b) presents the comparison between the test and simulation of the acceleration response under heel-drop excitations, with an error of less than 10% for the peak acceleration. This demonstrated that the model accurately simulated the peak acceleration response and attenuated trend.

4.3. Parameter Analysis. The parameters of the concrete filling range of the tree-like columns and the height-to-span ratio were critical factors that impacted the natural frequency and vibration response of pedestrian bridge bridges. The evaluation of the impact of these two parameters on the dynamic characteristics and vertical response of pedestrian bridges assessed the comfort and durability of the bridges under various structural schemes, providing reference and recommendations for practical design.

4.3.1. Effect of Depth-to-Span Ratio. Parametric analysis was conducted on pedestrian bridges with height-to-span ratios ranging from 1/20 to 1/80. The effect of the height-to-span ratio on the vertical fundamental frequency and peak acceleration of the bridges was investigated.

Table 3: Comparison of finite element simulation and experimental values.

	Frequency		Peak acceleration
Experiment	3.35 Hz	7.64 Hz	0.38 m/s^2
Finite element	3.38 Hz	7.34 Hz	0.44 m/s^2
Experiment/finite element	0.99	1.04	0.86

As depicted in Figure 9(a), the relationship between the height-to-span ratio and fundamental frequency was established. The results indicated that an increase in the height-to-span ratio leads to an increase in the fundamental frequency of the bridge. A 66.33% increase in the fundamental frequency was observed when the height-to-span ratio increased from 1/80 to 1/40. Furthermore, a significant rise in the fundamental frequency was observed when the height-to-span ratio increased from 1/40 to 1/20, with a value of 5.94 Hz rising to 21.49 Hz. It is worth noting that when the height-to-span ratio was 1/80, the fundamental frequency of the pedestrian bridge was only 2.01 Hz, which falls below the 3 Hz requirement specified in the CJJ-69 code, necessitating measures to improve the stiffness and damping of the pedestrian bridge.

Figure 9(b) presents the results of the peak vertical acceleration at various locations under heel-drop excitations. The results showed that an increase in the height-to-span ratio from 1/80 to 1/20 led to a 37.52% decrease in the peak acceleration in the mid-span of the bridge under single-person excitations. This highlights the significant impact of the height-to-span ratio on both the vertical fundamental frequency and peak acceleration of pedestrian bridges. Larger height-to-span ratios result in higher fundamental frequencies and lower acceleration responses.

4.3.2. Effect of Concrete-Filling Range of Tree-like Columns. Figure 10 shows five different concrete filling ranges I to V. Figure 11(a) provides the variation curve of the pedestrian

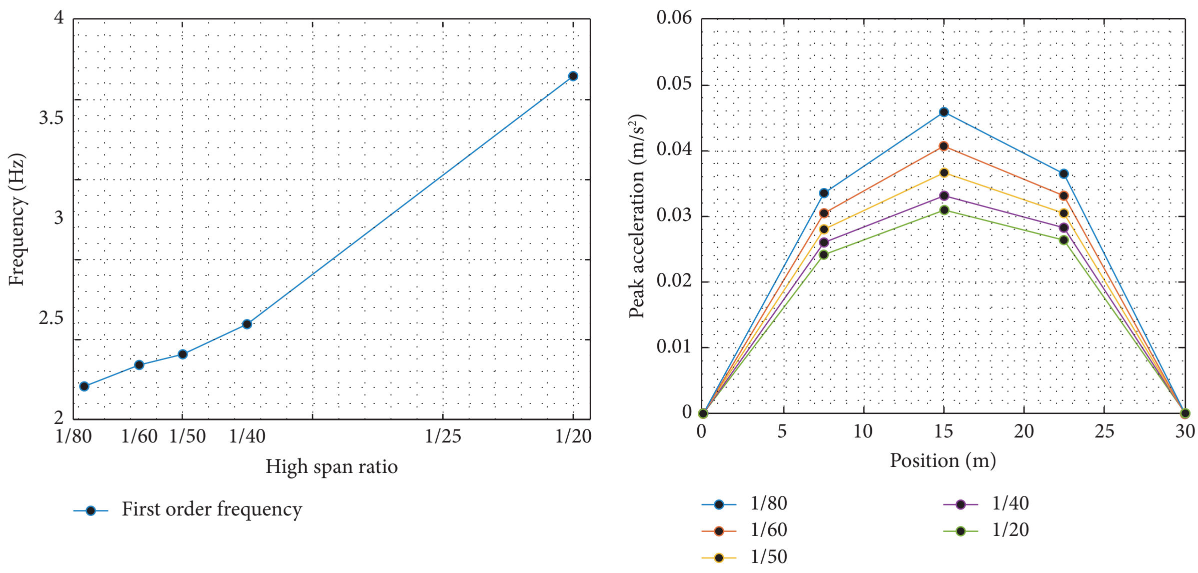

Figure 9: Analysis of pedestrian bridge height-to-span ratio parameters: (a) fundamental frequency and (b) peak acceleration.

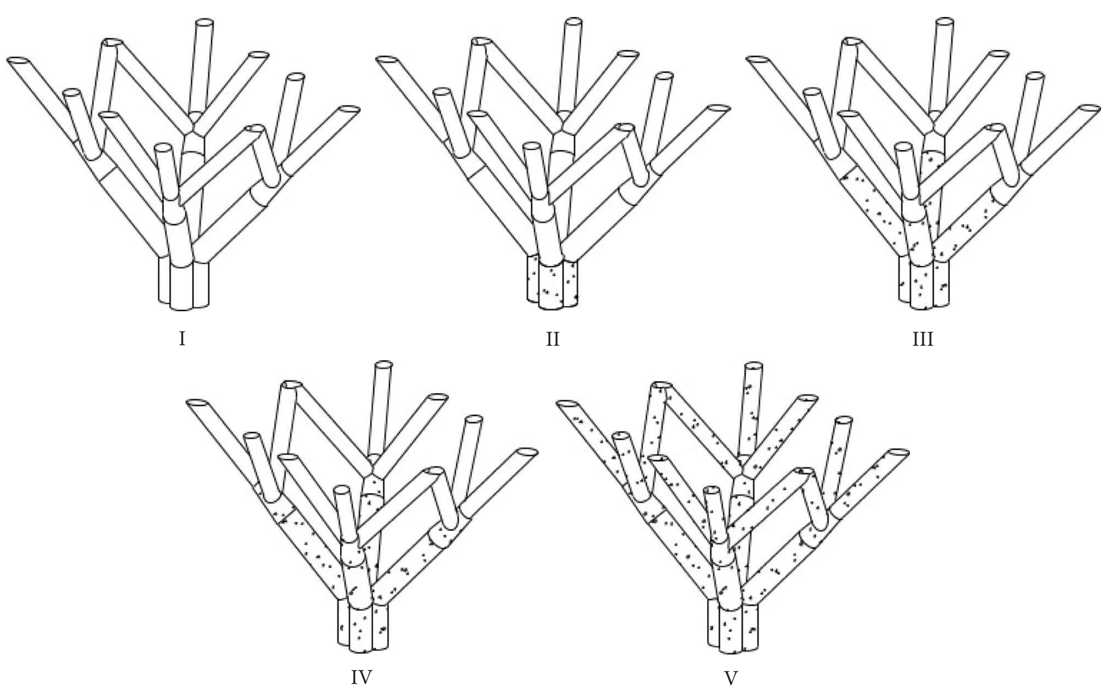

Figure 10: Five filling ranges of concrete.

bridge's natural frequency with the change in concrete filling range. As seen in the figure, the natural frequency of the pedestrian bridge gradually increased as the concrete filling range increased. Compared to the case without concrete filling, the natural frequency of the pedestrian bridge increased by 2.53%, 6.96%, 8.86%, and 9.73% for four different concrete filling ranges, respectively. However, this increase was not significant, primarily due to the large span of the pedestrian bridge, which is mainly controlled by the steel box beam above. Under all concrete filling ranges, the natural frequency of the pedestrian bridge met the requirement specified in the CJJ-69 code, which states that it should be above 3 Hz.

Figure 11(b) illustrates the relationship between the vertical peak acceleration at various locations on the bridge and the concrete filling range under mid-span heel-drop excitations. As the concrete filling range increased from I to III, the peak acceleration in the mid-span of the bridge is decreased by 27.08%. However, when it further increased to IV, the decrease was only 9.67%. This indicates that to

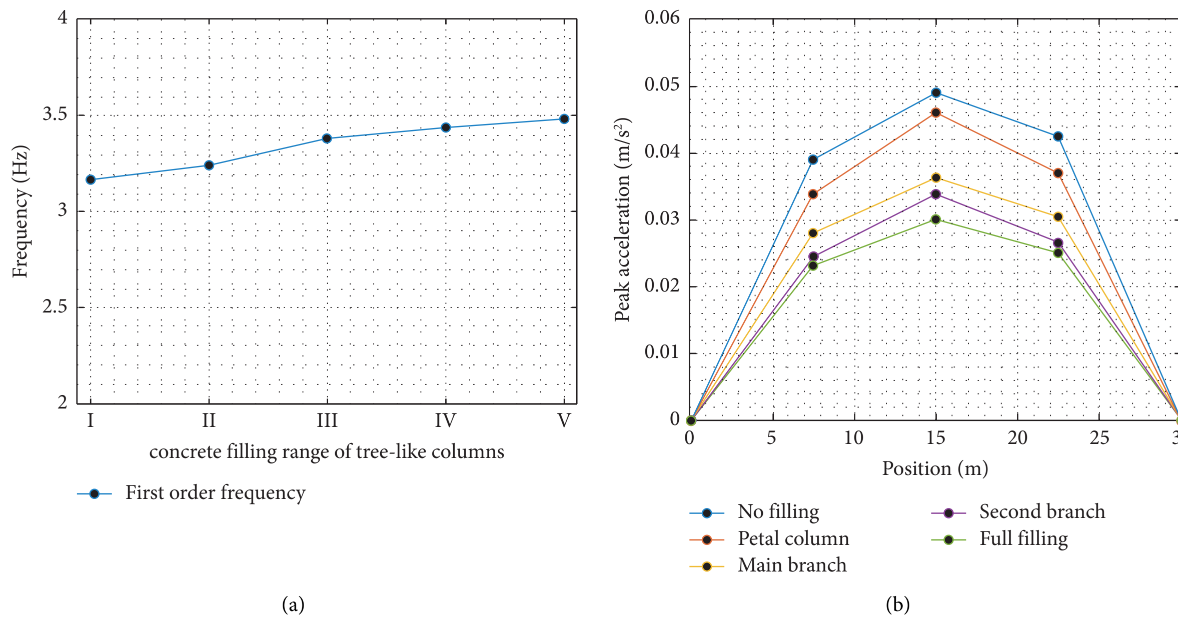

Figure 11: Analysis of concrete filling height parameters in pier column: (a) fundamental frequency and (b) peak acceleration.

a certain extent, increasing the concrete filling range of the tree-like columns could effectively reduce the vertical response of the pedestrian bridge and improved the structural comfort.

5. Simplify Heel-Drop Loading

To predict the vibration response of a pedestrian bridge under heel-drop excitations, two different heel-drop load models were employed in finite element analysis. The first was the idealized triangular load model proposed by Murray [14], as illustrated in Figure 12(a). This model assumed that only the heel strike moment generated an impact force during the heel-drop process, with a peak load of 3.14 times the body weight and a duration of 0.05 seconds. The second was the simplified heel-drop load model obtained from statistical analysis of measured data in this study, as shown in Figure 12(b). This model simplified the heel-drop load curve into two stages: from the body's zero position, when it maintained balance, to the peak point when the heel struck (t_1), and from the peak point to the load zero position, when the body vibrated (t_2). The model normalized the weight of the test subject and considered the correlation between the load peak and body weight, with a peak load of 2.59 times the body weight. The average duration of the rising and falling segments was 0.025 seconds and 0.071 seconds, respectively.

In this paper, the heel-drop load was simplified to the following equation:

$$F(t) = \begin{cases} 105.1Gt - 102.5G\ (0 \leq t \leq 0.025) \\ -36.9Gt + 39.5G\ (0.025 \leq t \leq 0.735) \\ 0\ (t < 0 \text{ or } t > 0.735), \end{cases} \tag{2}$$

where G = the body weight, and t = the time.

The two models of heel-drop loads were input into the finite element model and compared to the recorded acceleration time histories. Figures 13(a) and 13(b) show the comparison between the vertical acceleration time histories obtained from the use of the two heel-drop load models and the recorded data. The red and black curves indicated the acceleration time histories obtained from simulation and measurement, respectively. It was evident that when the triangular load model proposed by Murray was used, the simulated peak acceleration was significantly higher than the recorded result, with a relative error of 24.6%. This was because the Murray model only considered the impact of the human heel-drop and overlooked the changes in load during the human balancing and vibration process. However, when the simplified heel-drop load model based on statistical data from recorded data was used, the simulated result was in close agreement with the recorded result, with a relative error of 9%. It could be concluded that the simplified heel-drop load model proposed in the study better reflected the load characteristics of the human heel-drop process.

5.1. Peak Coefficient between Accelerated Response Heel-Drop Walking.

The vibrations of a pedestrian bridge were obtained through heel-drop excitations tests. However, in practical engineering, pedestrian bridges are more commonly subjected to walking excitations. To establish the relationship between the structural peak acceleration response under heel-drop excitations and walking excitations, a peak acceleration coefficient β was proposed based on the peak acceleration at the mid-span position of the bridge for both excitation types and different step frequencies.

Table 4 presents the average peak acceleration at the mid-span of the pedestrian bridge for five testers under three heel-drop excitations. This served as a reference for comparison with the structural peak acceleration differences

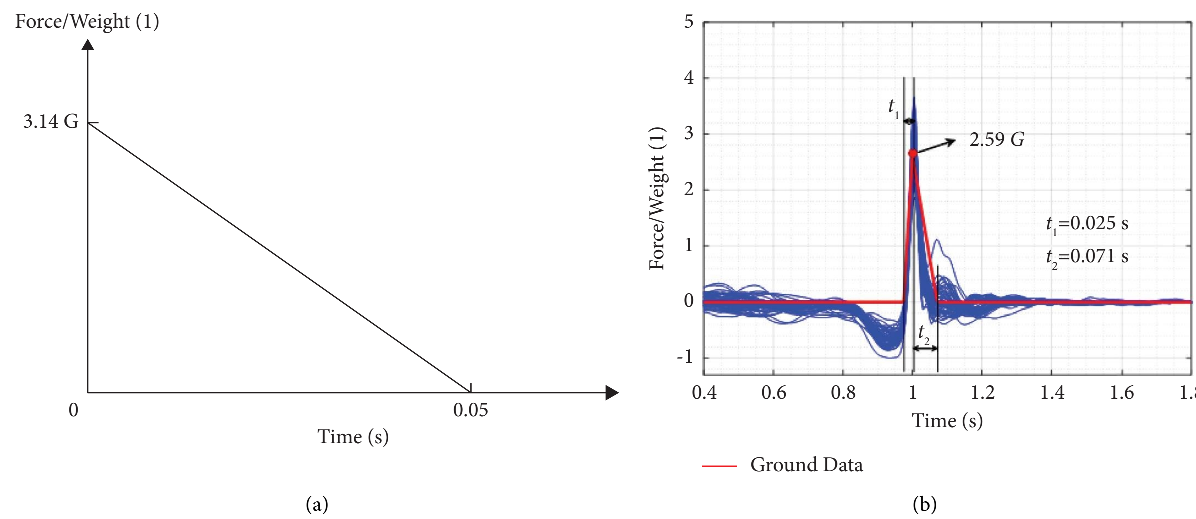

Figure 12: (a) Murray simplified heel-drop load and (b) simplified heel-drop load in this paper.

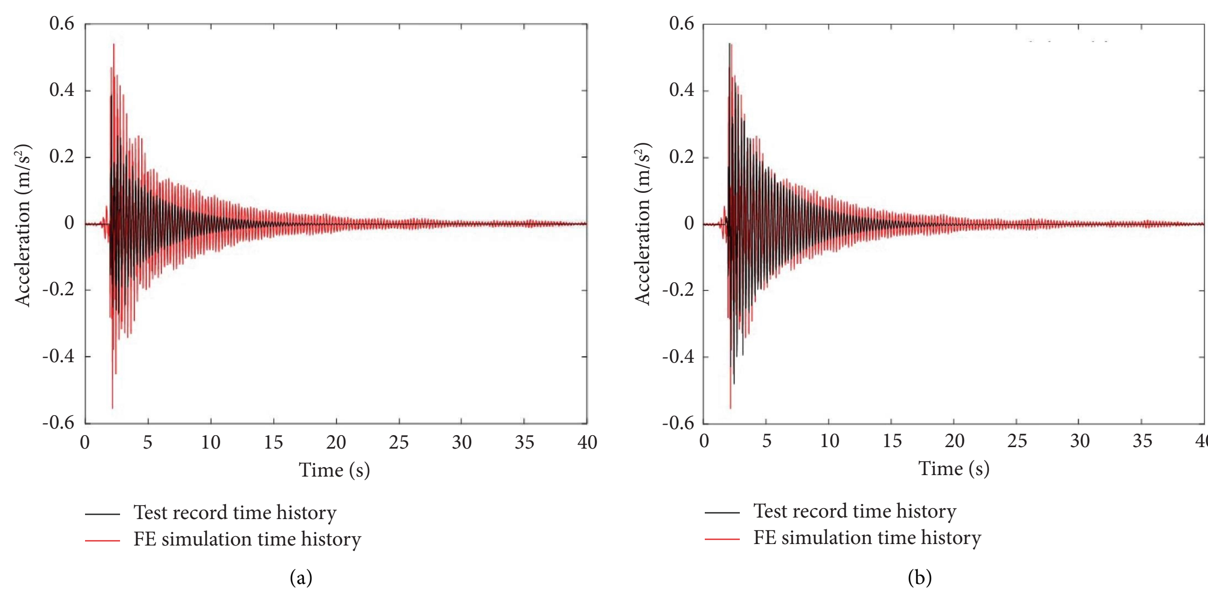

Figure 13: (a) Simulated acceleration under Murray heel-drop load and (b) simulated acceleration under simplified heel-drop load in this paper.

Table 4: Peak acceleration in the span of heel-drop with different weights.

Tester no.	V1	V2	V3	V4	V5
Body weight (kg)	59	65	82	85	60
Peak acceleration (m/s^2)	0.187	0.193	0.236	0.293	0.316

under walking excitations with various step frequencies for the same individuals. The corresponding peak coefficients β were then calculated. β was defined as the ratio of the peak acceleration due to the heel-drop load to the peak acceleration caused by the walking load.

$$\beta = \frac{a_H}{a_W}, \tag{3}$$

where a_H = the peak acceleration (m/s^2) caused by the heel-drop, and a_W = the peak acceleration (m/s^2) caused by the walking load.

Figure 14(a) illustrated the distribution of the peak coefficient β, which was derived by normalizing the test subject's weight for various step frequencies. The peak coefficient β was found to lie within the range of 1.5 to 2.5, and the results demonstrated a linear decline in the peak coefficient β as the step frequency increased. Employing Grubbs' principle [41], the distribution of the peak coefficient was determined under the detection level condition $\alpha_{\_lev} = 0.05$. When the step frequency equaled 1.7 Hz, the mean peak acceleration coefficient β, under heel-drop excitations, registered at 1.95, accompanied by a standard deviation of 0.192. At a step frequency of 2.0 Hz, the mean

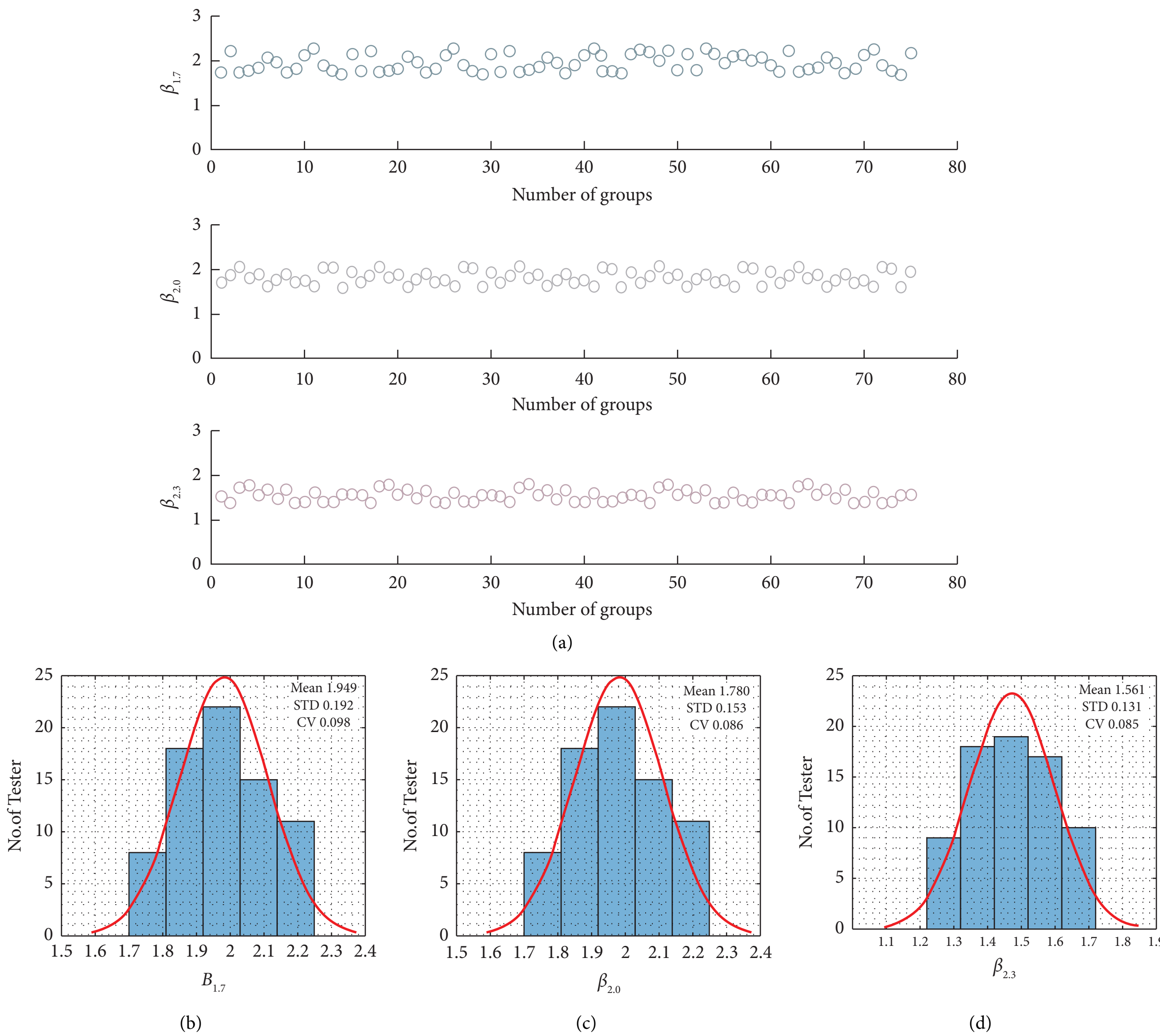

Figure 14: (a) Histogram of coefficient β distribution, (b) coefficients β for walk 1.7 Hz, (c) coefficients β for walk 2.0 Hz, and (d) coefficients β for walk 2.3 Hz.

coefficient β was measured at 1.78, with a standard deviation of 0.153. Finally, when the step frequency reached 2.3 Hz, the mean coefficient β stood at 1.56, accompanied by a standard deviation of 0.131, as depicted in Figures 14(b)–14(d).

5.2. Discussion of Peak Coefficient. To verify the accuracy of the peak acceleration coefficients, the coefficients at different step frequencies were analyzed in this study based on finite element and experimental results. In performing the theoretical analysis on the dynamic response due to walking excitations, the factors of human weight and the duration of single-step excitation were considered, which were also considered to develop the walk forcing function. As a result, the following Fourier series [42] defining the single-step walk forcing function $F(t)$ was derived, as shown in Figure 15(a). For the single-step walking considered in the previous study, the first six terms ($n = 1$–6) of the series were developed based on the experimental observations. With the increase of n, the simulation accuracy of the formulation is enhanced. Higher orders of harmonics ($n = 3$–6) were considered in the derivation, and typical measured and predicted force-time histories from Participant 1 are shown in Figure 14(a). Compared with the test results, Figure (4) shows a better accuracy with $n = 6$ for directions z (vertical directions) [43]. Therefore, the single-step walk forcing functions $F(t)$ can be modified as follows:

$$F(t) = G\left[\alpha_0 + \sum_{i=1}^{6} \alpha_i \sin\left(\frac{2i\pi}{T_p} t + \varphi_i\right)\right] \text{for direction } z. \quad (4)$$

In this study, the peak response of the pedestrian bridge under single-step walking excitation was well-fitted by the finite element model using the input from (4), as shown in

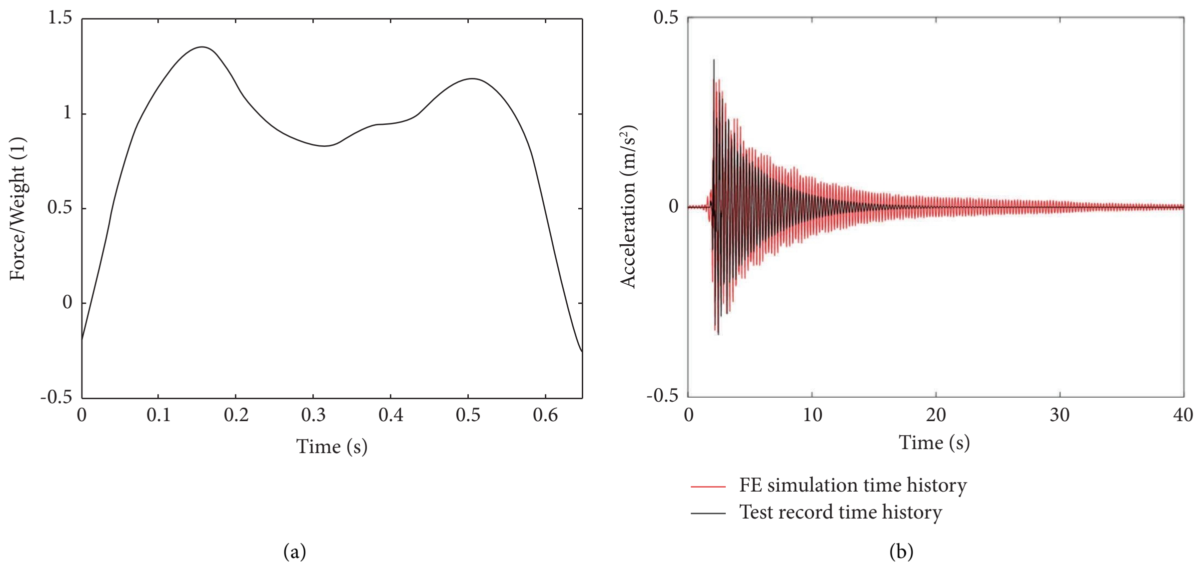

Figure 15: (a) Single walking load (b) Simulated acceleration under single walking load in this paper.

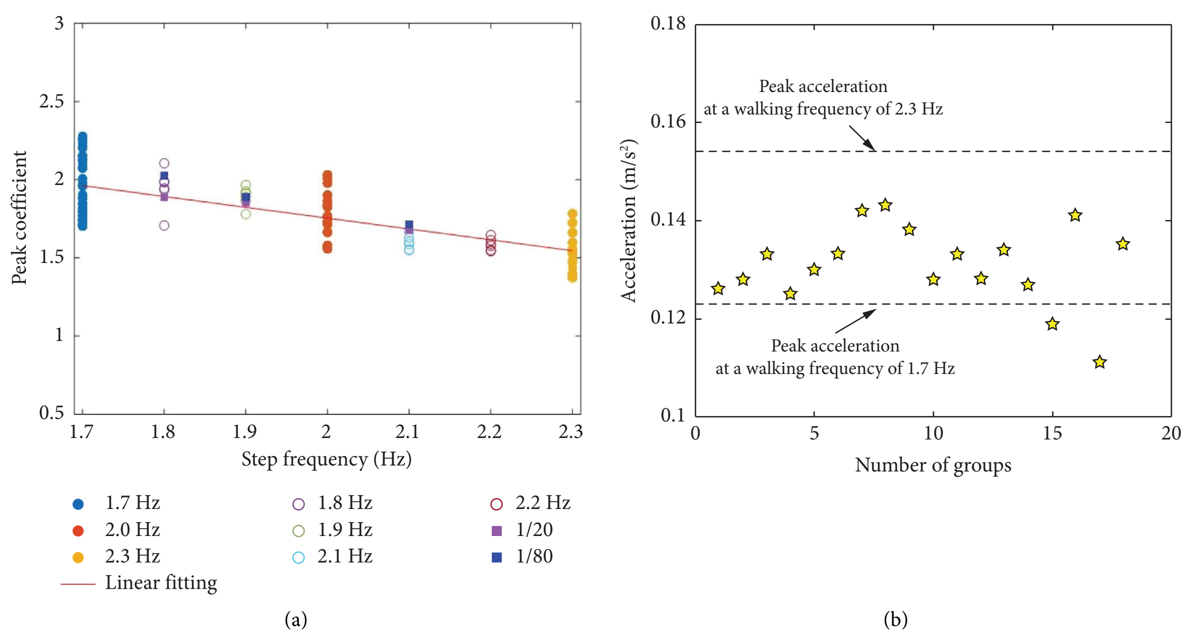

Figure 16: (a) Coefficients β under common step frequency and (b) coefficients β under random step frequency.

Figure 15(b). The trend of the coefficients of low height-to-span ratio pedestrian bridges at different step frequencies was analyzed. At a frequency of 1.7 Hz, heel-drop loading produced peak acceleration that was approximately 1.95 times greater than that caused by walking load. As the frequency increased to 2.3 Hz, the peak acceleration resulting from the heel-drop load was observed to be approximately 1.56 times higher than that induced by the walking load. In addition, the finite element model analysis was conducted to determine the peak acceleration for various step frequencies of footfall and walking loads on the pedestrian bridge at 1/20 and 1/80 high span ratios. The analyses revealed a similar coefficient relationship between these variables, as shown in Figure 16(a). The peak coefficients of the acceleration responses for both heel-drop and walking loads exhibited a linear decrease with increasing walking frequency, as shown in the following equation:

$$\beta = -0.7f + 3.14 \; (1.7 \le f \le 2.3), \quad (5)$$

where β = the Peak coefficient, and f = step frequencies (Hz).

The 2nd tester, weighing 65 kg, was selected for the analysis. The tester's heel-drop load time history was obtained by incorporating it into the simplified heel-drop load model, which yielded a peak acceleration of 0.24 m/s^2 for the bridge under heel-drop excitations. The peak acceleration of the bridge under walking excitations with step frequencies of

1.7 Hz and 2.3 Hz was then calculated using the peak acceleration coefficients $\beta_{1.7}$ and $\beta_{2.3}$, resulting in values of 0.12 m/s^2 and 0.15 m/s^2, respectively. Figure 16(b) presents the relationship between the peak acceleration of the bridge obtained from the measured walking (random step frequency) and the equivalent peak acceleration of 1.7 Hz and 2.3 Hz step frequency calculated. It was observed that 89% of the measured peak acceleration data during actual walking fell within the calculated limit value, indicating a high degree of reliability for the peak coefficient. Moreover, 11% of the measured peak acceleration data under actual walking was lower than the peak acceleration at the 1.7 Hz step frequency. This phenomenon occurred because pedestrians decelerate their walking frequency to maintain comfort during continuous walking [44]. No data exceeded the structural peak acceleration corresponding to the 2.3 Hz walking frequency. This demonstrated that the proposed coefficient can effectively predict the structural peak acceleration under different single-person step frequencies for walking excitations. In general, it was observed that the walking frequency of pedestrians ranged from 1.7 Hz to 2.3 Hz. Consequently, the utilization of $\beta_{1.7}$ and $\beta_{2.3}$ proved to be effective in estimating the acceleration response of the bridge under different walking frequencies.

6. Conclusion

The vibration characteristics and acceleration responses of pedestrian bridges were examined in this study through a combination of field experiments and finite element analysis. The primary conclusions derived from the study are as follows:

(1) The responses of both heel-drop and walking excitations were effective in obtaining the fundamental frequency of the pedestrian bridge. Moreover, the damping obtained from heel-drop excitations was found to be more stable compared to that obtained from walking excitations. The average damping ratio under walking load was 0.022, while the average damping ratio measured under heel-drop load was 0.018. On-site experiments under environmental excitations revealed that the vertical fundamental frequency of the pedestrian bridge was 3.35 Hz, with a damping ratio of 0.018.

(2) Finite element analysis revealed that reduced height-to-span ratios correspond to lower fundamental frequencies and increased acceleration responses. With a ratio of 1/80, the pedestrian bridge's fundamental frequency was 2.01 Hz, below the 3 Hz minimum specified by the CJJ69-95 code, necessitating stiffness, and damping improvements. Furthermore, the fundamental frequency's increase due to varying tree pier concrete filling ranges was not substantial. As the concrete filling range escalated from I to III, the bridge's mid-span peak acceleration dropped by 27.08%. This effectively reduced the vertical response of the bridge and enhanced its vibration serviceability.

(3) A simplified model for heel-drop load, as described by equation (2), was proposed to facilitate the easy evaluation of structural vibrations by designers. The peak coefficients of the acceleration responses for both heel-drop and walking loads exhibited a linear decrease with increasing walking frequency, as described by equation (5). At the step frequency of 1.7 Hz, heel-drop loading generated peak acceleration approximately 1.95 times greater than that caused by walking load. As the step frequency increased to 2.3 Hz, the peak acceleration resulting from the heel-drop load was found to be roughly 1.56 times higher than that induced by the walking load.

Data Availability

The data used to support the findings of this study are available from the corresponding author upon request.

Conflicts of Interest

The authors declare that there are no conflicts of interest.

Authors' Contributions

Wei Wang and Rui An contributed equally to this work.

Acknowledgments

This study was supported by the National Natural Science Foundation of China (Grant no. 51668053). The valuable contributions of Professor Gan Dan at Chongqing University are gratefully acknowledged.

References

[1] S. Y. Chen, F. Deng, Y. Huang, X. Jia, Y. P. Liu, and S. J. C. Lai, "bioOTU: An Improved Method for Simultaneous Taxonomic Assignments and Operational Taxonomic Units Clustering of 16s rRNA Gene Sequences," *Journal of computational biology: a journal of computational molecular cell biology*, vol. 23, no. 4, pp. 229–23839, 2016.

[2] P. Dallard, T. Fitzpatrick, A. Flint et al., "London Millennium Bridge: pedestrian-induced lateral vibration," *Journal of Bridge Engineering*, vol. 6, pp. 412–4177, 2001.

[3] J. M. Brownjohn, O. A. Hasan, and C. A. Taylor, "Response of the Bob Kerrey pedestrian bridge to crowd loading," *Journal of Bridge Engineering*, vol. 15, pp. 612–623, 2010.

[4] Y. Fujino, B. M. Pacheco, and S. Nakamura, "Study on the dynamic interaction of pedestrian and footbridges," *Earthquake Engineering & Structural Dynamics*, vol. 22, pp. 813–824, 1993.

[5] F. Venuti and A. Lamaro, "A new pedestrian bridge in Brisbane: the Kurilpa Bridge," *Structural Engineering International*, vol. 20, pp. 296–300, 2010.

[6] F. Venuti, F. Tubino, and F. Tubino, "Human-induced loading and dynamic response of footbridges in the vertical direction due to restricted pedestrian traffic," *Structure and Infrastructure Engineering*, vol. 17, no. 10, pp. 1431–144545, 2021.

[7] S. Zivanovic, A. Pavic, P. Reynolds, and P. Reynolds, "Vibration serviceability of footbridges under human-induced excitation: a literature review," *Journal of Sound and Vibration*, vol. 279, no. 1-2, pp. 1–74, 2005.

[8] R. L. Pimentel, *Vibrational Performance of Pedestrian Bridges Due to Human-Induced Loads*, Ph.D. thesis, University of Sheffield, Sheffield, United Kingdom, 1997.

[9] L.-L. Xie, S.-Y. Chen, A.-Q. Li, N. Zhang, and X. Zhou, "Human-induced loading and dynamic response of footbridges in the restricted traffic condition," *Human-Computer Interaction*, vol. 35, pp. 341–355, 2021.

[10] A. Kareem and T. Kijewski-Correa, *Pedestrian-Structure Interaction: Vibration Sensitivity and Mitigation. Pedestrian and Evacuation Dynamics*, Springer, New York, NY, USA, 2012.

[11] AISC AISC, *Design Guide 11: Vibrations of Steel-Framed Structural Systems Due to Human Activity*, American Institute of Steel Construction, Chicago, Illinois, USA, 2016.

[12] J. Ohmart, "Vibration serviceability of steel floor systems," *Engineering Journal*, vol. 51, pp. 61–73, 1968.

[13] T. M. Murray, "A triangular load function for the design of pedestrian walkways," *Engineering Structures*, vol. 3, pp. 53–59, 1975.

[14] S. Živanović, "Benchmark footbridge for vibration serviceability assessment under the vertical component of pedestrian load," *Engineering Structures*, vol. 32, pp. 3512–3521, 2010.

[15] C. Bedon, "Experimental investigation on vibration sensitivity of an indoor glass footbridge to walking conditions," *Journal of Building Engineering*, vol. 29, Article ID 101195, 2020.

[16] F. Venuti, V. Racic, A. Corbetta, and A. Corbetta, "Modelling framework for dynamic interaction between multiple pedestrians and vertical vibrations of footbridges," *Journal of Sound and Vibration*, vol. 379, pp. 245–26363, 2016.

[17] Z. O. Muhammad and P. Reynolds, "Probabilistic multiple pedestrian walking force model including pedestrian inter- and intrasubject variabilities," *Advances in Civil Engineering*, vol. 2020, Article ID 9093037, 14 pages, 2020.

[18] A. Mohammed, A. Pavic, V. Racic, A. Pavic, and V. Racic, "Improved model for human induced vibrations of high-frequency floors," *Engineering Structures*, vol. 168, pp. 950–96666, 2018.

[19] K. Van Nimmen, G. Lombaert, G. De Roeck, P. Van den Broeck, G. De Roeck, and P. Van den Broeck, "The impact of vertical human-structure interaction on the response of footbridges to pedestrian excitation," *Journal of Sound and Vibration*, vol. 402, pp. 104–12121, 2017.

[20] C. Caprani, E. C. Ahmadi, and E. Ahmadi, "Formulation of human–structure interaction system models for vertical vibration," *Journal of Sound and Vibration*, vol. 377, pp. 346–36767, 2016.

[21] E. Shahabpoor, A. Pavic, V. Racic, and V. Racic, "Structural vibration serviceability: Structural vibration serviceability: New design framework featuring human-structure interactionew design framework featuring human-structure interaction," *Engineering Structures*, vol. 136, pp. 295–311, 2017.

[22] C. Middleton, J. J. Brownjohn, and J. M. W. Brownjohn, "Response of high frequency floors: Response of high frequency floors: A literature review literature review," *Engineering Structures*, vol. 32, no. 2, pp. 337–35252, 2010.

[23] J. Santos, P. Andrade, P. Escórcio, and P. Escórcio, "Pre-design of laterally supported stair steps," *Engineering Structures*, vol. 182, pp. 51–61, 2019.

[24] C. Bedon, E. Bergamo, M. Izzi, S. Noè, M. Izzi, and S. Noè, "Prototyping and Prototyping and Validation of MEMS Accelerometers for Structural Health Monitoring—The Case Study of the Pietratagliata Cable-Stayed Bridgealidation of MEMS accelerometers for structural health monitoring—the case study of the pietratagliata cable-stayed bridge," *Journal of Sensor and Actuator Networks*, vol. 7, no. 3, p. 30, 2018.

[25] C. Bedon, M. Fasan, S. Noè, and S. Noè, "Body Body Motion Sensor Analysis of Human-Induced Dynamic Load Factor (DLF) for Normal Walks on Slender Transparent Floorsotion sensor analysis of human-induced dynamic load factor (DLF) for normal walks on slender transparent floors," *Journal of Sensor and Actuator Networks*, vol. 11, no. 4, p. 81, 2022.

[26] E. T. Ingólfsson, C. T. Georgakis, and J. Jónsson, "The influence of pedestrian walking patterns on the dynamic properties of pedestrian structures," *Journal of Bridge Engineering*, vol. 17, pp. 913–922, 2012.

[27] Y. Fujino, B. M. Pacheco, and S. Nakamura, "Dynamic interaction between pedestrians and a flexible footbridge: a practical approach for analysis and design," *Structural Engineering/Earthquake Engineering*, vol. 10, pp. 31s–40s, 1993.

[28] J. Cooley, J. W. W. Tukey, and J. W. Tukey, "An algorithm for the machine calculation of complex Fourier series," *Mathematics of Computation*, vol. 19, no. 90, pp. 297–301, 1965.

[29] J. Bu-yu, Y. Xiao-lin, Y. Quan-sheng, Y. Zheng, Q. Yan, and Z. Yang, "Nonlinear Nonlinear Stochastic Analysis for Lateral Vibration of Footbridge under Pedestrian Narrowband Excitationtochastic analysis for lateral vibration of footbridge under pedestrian narrowband excitation," *Mathematical Problems in Engineering*, vol. 2017, Article ID 5967491, 12 pages, 2017.

[30] M. Bocian, J. H. G. Macdonald, and J. F. Burn, "Guidance for footbridge design: a new simplified method for the accurate evaluation of the structural response in serviceability conditions," *Advances in Bridge Engineering*, vol. 2, pp. 1–17, 2017.

[31] J. Zhang, X. Zhang, and Z. Wang, "An improved half-power bandwidth method for damping identification in structures," *Journal of Sound and Vibration*, vol. 399, pp. 150–165, 2017.

[32] Journey Machine learning, *Random Patches and Random Subspaces*, Machine Learning Journey, Phoenix, Arizona, 2020.

[33] D. Inaudi and I. F. C. Smith, *Guideline for the Design of Footbridges*, International Association for Bridge and Structural Engineering (IABSE), Zürich, Switzerland, 2005.

[34] H. Wu and H. Ji, "Damping ratio estimation of mechanical systems using the half-power bandwidth method: a review and new insights," *Mechanical Systems and Signal Processing*, vol. 123, pp. 37–59, 2019.

[35] A. Gheitasi, O. E. Ozbulut, S. Usmani et al., "Experimental and analytical vibration serviceability assessment of an in-service footbridge," *Case Studies in Nondestructive Testing and Evaluation*, vol. 6, pp. 79–88, 2016.

[36] Beijing Municipal Engineering Research, *Technical Specifications of Urban Pedestrian Overcrossing and Underpass*, Beijing Municipal Engineering Research, Beijing, China, 1995.

[37] D. Han, S. Wu, and X. Dai, "Study on the friction coefficient of steel-concrete interface under different load and roughness conditions," *Journal of Applied Sciences*, vol. 15, pp. 1314–1319, 2015.

[38] R. Kalyankar and V. Shinde, "Mesh convergence study for 3D finite element analysis of reinforced concrete (RC) deep beams," *International Journal of Advanced Engineering Research and Science*, vol. 4, pp. 1–8, 2017.

[39] J. M. W. Brownjohn and T. N. Fu, “Vibration excitation and control of a pedestrian walkway by individuals and crowds,” *Shock and Vibration*, vol. 12, pp. 357–368, 2005.
[40] C. Bedon, “Diagnostic analysis and dynamic identification of a glass suspension footbridge via on-site vibration experiments and FE numerical modelling,” *Composite Structures*, vol. 216, pp. 366–37878, 2019.
[41] F. E. Grubbs, “Sample criteria for testing outlying observations,” *The Annals of Mathematical Statistics*, vol. 21, no. 1, pp. 27–58, 1950.
[42] L. Cao and Y. F. Chen, “Formulation of human–structure interaction for vibration serviceability of steel–concrete composite floors,” *Structural Control and Health Monitoring*, vol. 28, Article ID e2679, 2021.
[43] L. Cao, J. Li, Y. Frank Chen, S. Huang, Y. F. Chen, and S. Huang, “Measurement and application of walking models for evaluating floor vibration,” *Structures*, vol. 50, pp. 561–57575, 2023.
[44] C. C. Caprani and P. Fanning, “Comfort assessment of pedestrians on footbridges subject to random vibration,” *Proceedings of the ICE-Bridge Engineering*, vol. 164, pp. 203–214, 2011.